Trees, Forests and People 20 (2025) 100853

Contents lists available at ScienceDirect

Trees, Forests and People

journal homepage: www.sciencedirect.com/journal/trees-forests-and-people

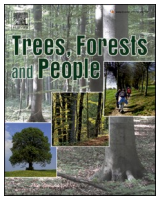

Physiological adaptations to different shade levels and their role in enhancing yield and quality of *Ficus formosana* Maxim. for under-forest economy: Insights from greenhouse and forest environments

Ping-Huan Tsai [a], Yao-Yu Chiang [b], Chih-Ming Lai [b], Hung-Chih Lin [b], Yao-Moan Huang [c], Tzu-Hao Su [b,*]

[a] *Department of Forestry, National Chung Hsing University, Taichung, 402202, Taiwan*
[b] *Silviculture Division, Taiwan Forestry Research Institute, Taipei, 100060, Taiwan*
[c] *Forest Ecology Division, Taiwan Forestry Research Institute, Taipei, 100060, Taiwan*

ARTICLE INFO

Keywords:
Understory
Abiotic stress
Light gradient
Edible plants
Antioxidant activity
Secondary metabolites

ABSTRACT

Ficus formosana Maxim., an emerging under-forest economic crop, adapts to understory environments but exhibits growth variations under different canopy and light conditions. This study analyzed the growth, physiological, and biochemical responses of *F. formosana* under three shading gradients in greenhouse and broadleaved forest environments to evaluate the effects of light intensity on plant performance. After eight months, plants in unshaded forest environments showed increased hydrogen peroxide and malondialdehyde levels and reduced Fv/Fm, indicating oxidative stress and photosystem damage. In contrast, severe shading promoted chlorophyll content, specific leaf area, and leaf area ratio, enhancing light capture, but restricted stomatal conductance and carbon assimilation, ultimately limiting metabolite production and biomass accumulation. Growth patterns in the greenhouse were consistent with those in the forest. However, physiological and morphological adaptations were observed across all shading conditions in the forest, highlighting the excellent shade tolerance and adaptive regulation of *F. formosana* in the understory environment. Optimal growth occurred under moderate shading, with 21 % relative light intensity and a daily light integral of ~4 mol photons m^{-2} day^{-1}, achieving the highest biomass and stable root secondary metabolite levels and DPPH scavenging activity. These findings underscore the critical role of optimizing light intensity in the cultivation of under-forest economic crops. For *F. formosana*, moderate shading provides the most favorable conditions for maximizing root yield, while simultaneously maintaining its antioxidant quality, thereby enhancing its economic viability.

1. Introduction

Agroforestry integrates agriculture and forestry to enhance land productivity, with forest farming emphasizing timber production and shade-tolerant non-timber forest products (NTFPs) to promote biodiversity and sustainability (Chamberlain et al., 2009; Pantera et al., 2021). As part of a broader effort to promote sustainable land use, Taiwan introduced the under-forest economy policy in 2019, a system similar to forest farming that focuses on the rational use of understory spaces and forest resources within sustainable limits (Chen, 2022; Xu, 2019). This policy emphasizes the cultivation of high-value NTFPs under existing forest canopies while adhering to the Four No Principles—no impact on tree growth, no soil disturbance, no chemical fertilizers, and no pesticides—to preserve forest ecosystems while boosting farmer incomes and reducing urban-rural disparities (Huang, 2018; Wu et al., 2020). *Ficus formosana* Maxim., known as Taiwan fig tree, is a shade-tolerant evergreen shrub native to Taiwan and Orchid Island, thriving in broadleaf forest understories (Jung and Yang, 2002; Kuo et al., 2021). Its roots, traditionally used in Taiwanese folk medicine, contain antioxidant, anti-inflammatory, and anti-tumor compounds, including sterols, chromenes, aldehydes, and flavonoids (Sheu et al., 2005; Huang et al., 2013). Adaptable to understory environments and suitable for container cultivation, *F. formosana* aligns well with the Four No Principles of under-forest economy in Taiwan, making it highly suitable for cultivation in managed understory environments. However, its increasing economic value has subjected wild populations to

* Corresponding author.
E-mail address: thsu@tfri.gov.tw (T.-H. Su).

https://doi.org/10.1016/j.tfp.2025.100853

Available online 7 April 2025

significant harvesting pressure, leading to a severe decline in numbers (Tzeng et al., 2005). To ensure both its sustainable utilization and conservation, Taiwan's Forestry and Nature Conservation Agency (FANCA) announced in early 2023 the inclusion of *F. formosana* as a key species for promotion under the under-forest economy initiative, ensuring both its sustainable utilization and conservation.

Understory cultivation faces challenges from complex light environments shaped by planting locations (e.g., forest edges, gaps) and overstory traits (e.g., canopy density, deciduousness). Shade-tolerant tree species can adjust their morphophysiological traits in response to varying light levels, modifying their leaf structure, photosynthetic capacity, and resource allocation to optimize growth and survival (Cifuentes and Moreno, 2022; Firmino et al., 2021). In low light, they develop shade-tolerance strategies such as increased specific leaf area (SLA) and biomass allocation to leaf expansion, but prolonged shading reduces photosynthesis, tissue development, plant height, root collar diameter (RCD), biomass, and carbohydrate content (De Almeida et al., 2019; Mathur et al., 2018; Poorter et al., 2019). Conversely, under excessive light, shade-tolerant species reduce SLA and Chl $a + b$ content to limit light absorption and lower ΦPSII to restrict photochemical utilization. If excess light energy is not dissipated via NPQ, reactive oxygen species (ROS) accumulate, causing oxidative damage and inhibiting growth (Pospisil, 2016; Szymańska et al., 2017). To counteract ROS, plants activate antioxidant enzymes (SOD, POD, CAT, APX) and produce phenolic compounds and flavonoids, which neutralize ROS and absorb UV radiation to minimize tissue damage (Garcia-Caparros et al., 2021; Morales et al., 2010). In *F. formosana*, secondary metabolite accumulation plays a crucial role not only in its antioxidant capacity but also in its functional food potential. Since light availability strongly influences the production of these metabolites, understanding how different light conditions regulate their accumulation is essential for optimizing its cultivation and enhancing its health-related benefits.

Understanding the niche resource requirements of tree species is crucial for selecting crops and optimizing spatial arrangements in agroforestry to enhance resource efficiency and ecosystem resilience (Young, 2017). Since shade tolerance strongly influences species selection and spatial configuration, it is commonly assessed using methods such as light-response curves, successional seral stages, and species abundance along light gradients (Feng et al., 2018). A frequent approach involves testing species' growth under varying light conditions, often by comparing full-light and single-shading treatments. For instance, maple species exhibited greater height growth under shade (Sanford et al., 2003), while shading was also found to enhance midday Fv/Fm in the leaves of late-successional trees (Krause et al., 2012). Light gradient experiments further clarify species' optimal growth conditions. Poorter (1999) demonstrated that shade-tolerant species achieved their highest mean relative growth rate of biomass at relative light intensities of 20–40 %. Similarly, moderate light has been shown to enhance root growth in planted seedlings within forest understories (García-Pérez et al., 2021). Given the significance of light availability in plant growth, identifying shading characteristics and crop light requirements is essential for optimizing species combinations and planting configurations, ultimately minimizing competition and maximizing resource use in agroforestry systems (Abbasi Surki et al., 2020).

F. formosana has been officially recognized as a legal crop for Taiwan's under-forest economy; however, its growth characteristics and physiological responses under varying light conditions remain insufficiently studied. While artificial shading in greenhouse settings provides a controlled environment for assessing light intensity effects, it often fails to replicate the complex biotic and abiotic interactions found in natural ecosystems, which are crucial in shaping plant phenotypic plasticity (Valladares et al., 2007). A meta-analysis highlights this limitation, revealing a weak correlation ($R^2 = 0.26$) between laboratory and field phenotypic data, underscoring the challenges of replicating natural conditions in controlled studies (Poorter et al., 2016). Therefore, to comprehensively understand the responses of *F. formosana* to light availability, this study integrates controlled greenhouse experiments to evaluate light-gradient effects with field observations to examine plant performance under natural environmental variability. Additionally, although the nutritional and medicinal properties of *F. formosana* roots have been studied, their biochemical composition and antioxidant capacity under different light conditions remain poorly understood. Light availability influences secondary metabolite accumulation and antioxidant capacity in both leaves and roots, yet root responses may differ and remain largely understudied. Most studies have focused on leaf biomass and biochemical accumulation, demonstrating that optimal light conditions enhance biomass production while maintaining adequate concentrations of secondary metabolites (Deng et al., 2012; Xu et al., 2014). In contrast, how light availability affects root biochemical composition remains unclear, highlighting the need for further investigation.

This study aims to characterize the light adaptation of *F. formosana* by analyzing its physiological and biochemical responses in leaves and roots under different shading conditions. The findings will provide practical guidance for optimizing its cultivation in under-forest systems. We hypothesize that: (1) *F. formosana* exhibits optimal growth performance under moderate shading; (2) morphological and physiological responses of seedlings to light conditions in a greenhouse may differ from those in a natural forest; and (3) suitable light conditions enhance root yield and sustain antioxidant capacity in *F. formosana*.

2. Materials and methods

2.1. Experimental design and locations

This study employed a two-factor experimental design to examine shading environments and shading levels (2 sites × 3 shade levels). The shading environments consisted of artificial shading in a greenhouse (G) and natural shading in a forest (F), while the shading levels included no shade (NS), moderate shade (MS), and severe shade (SS). The greenhouse site was conducted at the Beigou Nursery of National Chung Hsing University, Taichung City (24°04′39.4″N, 120°43′04.3″E; 75 m above sea level [ASL]). The greenhouse, approximately 4 m in height and covering an area of 100 m^2, was naturally ventilated with 20-mesh nylon screens on the front and back and covered with a 0.1 mm polyethylene film on top, providing ~60 % light reduction. Treatments in the greenhouse included GNS (greenhouse no shade), GMS (greenhouse moderate shade), and GSS (greenhouse severe shade). Artificial shading was achieved using black high-density polyethylene nets: one layer was applied on top for GMS, while two layers were applied on top and one around the sides for GSS.

The forest site was conducted in a secondary broadleaf forest at the Xinxian Experimental Station of the Taiwan Forestry Research Institute, New Taipei City (24°50′24.6″N, 121°32′01.4″E; 346 m ASL). The overstory (20–30 m tall) consisted of trees such as *Acacia confusa* Merr. (DBH: 45–60 cm), *Litsea acuminata* (Bl.) Kurata (DBH: ~20 cm), and *Machilus zuihoensis* Hayata (DBH: ~30 cm). The understory (10–16 m tall) included *Mallotus paniculatus* (Lam.) Muell.-Arg. (DBH: ~20 cm) and *Schefflera octophylla* (Lour.) Harms (DBH: ~27 cm), with an overall tree density of approximately 700 plants ha^{-1}. Forest treatments included FNS (forest no shade), FMS (forest moderate shade), and FSS (forest severe shade). FNS is located in an open area near the forest, with no canopy cover and direct sunlight exposure at midday. FSS is approximately 20 m from FNS and is completely shaded by the overstory canopy, receiving minimal light throughout the day. FMS is situated between these two sites, partially shaded by edge trees, with brief sunlight exposure in the morning.

2.2. Experimental materials and treatments

The experimental materials consisted of one-year-old *F. formosana* seedlings cultivated at the Liouguei Nursery of the Taiwan Forestry Research Institute (22°58′03.8″ N, 120°39′08.2″ E; 260 m ASL). The

seedlings were grown outdoors, with an average height of ~45 cm and a RCD of ~4 mm. In February 2023, uniform seedlings were selected and transferred to greenhouse and forest environments, both under ~60 % shade. Roots were pruned, and seedlings were repotted, followed by a 30-day acclimation period before the formal shading treatments began. Each shading treatment, in both greenhouse and forest settings, was randomly assigned 20 uniform seedlings (n = 20), totaling 120 seedlings.

In the greenhouse, seedlings were planted in 2.5 L square deep-rooted container (polypropylene [pp], dimensions: ~8.5 × 8.5 × 36 cm) to prevent root circling caused by vigorous growth. In contrast, forest seedlings, following policy guidelines, were planted in 2.5 L root-control pots (pp, diameter: 17.5 cm, height: 14 cm) and shallowly buried in the forest soil. The growth medium consisted of peat moss, perlite, vermiculite, and organic fertilizer (2:1:1:1, v/v/v/v). The organic fertilizer composition included nitrogen (2.5 %), phosphorus (2.5 %), potassium (1.5 %), and organic matter (60.0 %). Greenhouse seedlings were irrigated daily with tap water, while forest seedlings relied solely on rainfall to maintain practice relevance. The experiment spanned approximately eight months (231 days of experiment [DOE]), from March to November 2023.

2.3. Environmental monitoring

Photosynthetic photon flux density (PPFD) was measured every 5 min using quantum sensors (S-LIA-M003, Onset Computer Corp., Bourne, MA, USA) installed in greenhouse and forest environments under different shading treatments. Data were presented as 60 min moving averages. To capture cumulative light exposure while accounting for variations caused by instantaneous changes in PPFD, the recorded values (μmol m^{-2} s^{-1}) during photoperiods were summed and converted into the daily light integral (DLI, mol photons m^{-2} day^{-1}) (Kang et al., 2022) using the following equation:

$$DLI\ (\text{mol photon m}^{-2}\ \text{day}^{-1}) = \frac{\Sigma(PPFD \times 300\ \text{s})}{1000000}$$

The average relative light intensity (%) for each shading treatment across both sites was calculated as the mean DLI during the experimental period, relative to the DLI under no shade conditions. Temperature and relative humidity were recorded every 5 min using smart sensors with solar radiation shields (S-THB, Onset Computer Corp., Bourne, MA, USA) installed in unshaded areas of the greenhouse and forest. Data were presented as 60 min moving averages. Rainfall data for the forest site were obtained from the Tonghou Station of the Central Weather Administration (24°50′53.5″N, 120°35′52.8″E), located approximately 6.5 km from the forest site.

2.4. Growth performance and physiological investigations in the field

Seedling height, RCD, chlorophyll fluorescence, and stomatal conductance (g_s) were measured for all seedlings on the final day of the experiment. RCD was measured using a vernier caliper (mm), and seedling height was determined using a height ruler, measuring from the RCD mark to the terminal bud (cm) (n = 20). Chlorophyll fluorescence and g_s were measured on the 3rd, 4th, and 5th mature leaves using an LI-600 porometer/fluorometer (LI-COR Inc., Lincoln, Nebraska, USA), with the mean value recorded as the measurement for each seedling (n = 10). ΦPSII and g_s were measured at 11 a.m. after the seedlings were fully exposed to light, while the Fv/Fm was measured starting at 8 pm., following at least 3 h of natural dark adaptation, with measurements completed within approximately 1 h. ΦPSII was measured at 11 a.m. to avoid potential errors caused by direct sunlight at 10 a.m. in the FMS while ensuring consistency across all treatments and reflecting the light-adapted state under different light environments. In contrast, Fv/Fm was measured at night after natural dark adaptation to prevent potential heat accumulation caused by manually covering the leaves during the daytime. The LI-600 automatically calculated chlorophyll fluorescence parameters based on collected fluorescence signals. ΦPSII was determined from the steady-state fluorescence (F_s) and maximum fluorescence under light-adapted conditions (F_m'), while Fv/Fm was derived from the minimum fluorescence in the dark-adapted state (F_0) and maximum fluorescence after a saturating pulse (F_m). These values were obtained directly from the instrument.

2.5. Sample preprocessing for laboratory analysis

At the end of the experiment, 10 seedlings per treatment were randomly selected for destructive sampling and subsequent physiological and biochemical analyzes (n = 10). Roots and leaves were washed with double-distilled water before morphological growth parameters were measured. After measurements, 20 leaf discs (6.5 mm diameter) were randomly punched from each seedling's leaves for relative water content (RWC) analysis. The remaining leaves were finely chopped, thoroughly mixed, and divided into weighed portions according to the specific sample mass required for each analysis, then stored at −60 °C for further analysis.

2.6. Measurement of morphological parameters

Root length (cm) was measured using a measuring tape, from the root collar to the tip of the longest fine root. Total leaf area (cm^2) was determined by scanning all leaves from each seedling using a scanner, followed by summation of the areas calculated with ImageJ software (National Institutes of Health, Bethesda, MD, USA). Roots and stems were dried at 70 °C to a constant weight and weighed to determine dry weight. Leaf dry weight was calculated by drying the remaining leaves from physiological and biochemical analyzes and adjusting for water content and total fresh leaf weight. Total plant dry weight (g) was obtained by summing the dry weights of roots, stems, and leaves. SLA and leaf area ratio (LAR) were calculated using the following equations:

$$SLA\ (\text{cm}^2\ \text{g}^{-1}) = \frac{\text{Total leaf area}}{\text{Leaf dry weight}}$$

$$LAR\ (\text{cm}^2\ \text{g}^{-1}) = \frac{\text{Total leaf area}}{\text{Total plant dry weight}}$$

2.7. Measurement of physiological and biochemical parameters

2.7.1. RWC

Twenty fresh leaf discs were collected and weighed to obtain their fresh weight (W_1). The discs were then placed in tubes containing 15 mL of deionized water and soaked for 18 h. After soaking, the discs were blotted dry and weighed to determine their turgid weight (W_2). Finally, the discs were dried at 70 °C to a constant weight (W_3). RWC was calculated using the following equations:

$$RWC\ (\%) = \frac{(W_1 - W_3)}{(W_2 - W_3)} \times 100\%$$

2.7.2. Photosynthetic pigments

Frozen leaf samples (0.05 g) were ground into a powder with liquid nitrogen and extracted with 15 mL of 80 % acetone to isolate photosynthetic pigments. The extract was filtered through 1 μm pore-sized filter paper (Toyo Roshi Kaisha, Ltd., Tokyo, Japan), and the absorbance of the filtrate was measured at 470, 647, and 663 nm (A_{470}, A_{647}, and A_{663}) using a spectrophotometer (V730, Jasco Co., Tokyo, Japan). Chl a, Chl b, and Cars concentrations were calculated using the following equations and expressed as content per unit leaf dry weight (mg g^{-1} DW) (Lichtenthaler, 1987):

$$\text{Chl } a\ (\text{mg L}^{-1}) = 12.25 \times A_{663} - 2.79 \times A_{647}$$

$$\text{Chl } b \left(\text{mg L}^{-1}\right) = 21.50 \times A_{647} - 5.10 \times A_{663}$$

$$\text{Cars} \left(\text{mg L}^{-1}\right) = \frac{1000 \times A_{470} - 1.82 \times \textit{Chl a} - 85.02 \times \textit{Chl b}}{198}$$

2.7.3. Hydrogen peroxide and malondialdehyde

Frozen leaf samples (0.1 g) were ground with liquid nitrogen and extracted using 0.1 % trichloroacetic acid. After filtration and centrifugation, the supernatant was collected for analyzes. Hydrogen peroxide (H_2O_2) content was quantified based on absorbance at 390 nm after reaction with potassium iodide, following the method of Alexieva et al. (2001). Malondialdehyde (MDA) content was determined using the thiobarbituric acid assay, with absorbance measurements at 532 nm and 600 nm and calculations based on the extinction coefficient (Esterbauer and Cheeseman, 1990).

2.7.4. Soluble protein

Soluble protein content was quantified using the Bradford protein assay. Frozen leaf samples (0.05 g) were ground with liquid nitrogen and extracted with phosphate buffer (pH 7.0). After filtration and centrifugation, the supernatant was reacted with Coomassie brilliant blue G-250 reagent, and absorbance was measured at 595 nm. Soluble protein content (mg g^{-1} DW) was calculated using a standard curve prepared with bovine serum albumin (Bradford, 1976).

2.7.5. Antioxidant enzymes

Frozen leaf samples (0.2 g) were ground with liquid nitrogen and extracted using an enzyme extraction buffer. After filtration and centrifugation, the supernatant was used to measure the activities of POD (EC 1.11.1.7), APX (EC 1.11.1.11), and CAT (EC 1.11.1.6). POD activity was determined by monitoring the increase in absorbance at 470 nm using guaiacol as a substrate (Chance and Maehly, 1955). APX activity was measured based on the decrease in absorbance at 290 nm, reflecting ascorbic acid consumption (Nakano and Asada, 1981). CAT activity was evaluated by recording the decrease in absorbance at 240 nm due to H_2O_2 breakdown (Aebi, 1984). Enzyme activities were expressed as U mg^{-1} protein.

2.7.6. Soluble sugars and starch

For soluble sugar extraction, 0.05 g of oven-dried leaf powder or 0.1 g of oven-dried root powder was mixed with deionized water and extracted twice in an 80 °C water bath, followed by centrifugation to collect the combined supernatants, which were diluted to 50 mL. Starch extraction was performed on the residue using perchloric acid, with the combined extracts diluted to 50 mL. Soluble sugar and starch contents were quantified using the phenol-sulfuric acid method, with absorbance measured at 485 nm and calculations based on a glucose standard curve (DuBois et al., 1956). Results were expressed as mg g^{-1} DW.

2.7.7. TPC, TFC, and DPPH-RSA

For the extraction of TPC and TFC, 0.05 g of oven-dried leaf powder was extracted with 47.5 % ethanol in an 80 °C water bath for 60 min, diluted to 50 mL, and centrifuged to collect the supernatant. Similarly, 0.1 g of oven-dried root powder was extracted with deionized water, diluted to 20 mL, and centrifuged to collect the root supernatant. TPC was determined using the Folin-Ciocalteu method, with absorbance measured at 765 nm and results expressed as mg gallic acid g^{-1} DW (Singleton and Rossi, 1965). TFC was measured with an $AlCl_3{\cdot}6H_2O$ reaction, with absorbance recorded at 415 nm and results expressed as mg quercetin g^{-1} DW (Chang et al., 2002). 2,2-Diphenyl-1-picrylhydrazyl radical scavenging activity (DPPH-RSA) was calculated by comparing absorbance at 517 nm between control, sample, and blank treatments, and expressed as a percentage of radical scavenging activity (Brand-Williams et al., 1995):

$$\text{DPPH...RSA } (\%) = \frac{A_{control} - \left(A_{sample} - A_{blank}\right)}{A_{control}} \times 100\%$$

where $A_{control}$, A_{sample}, and A_{blank} represent the absorbance of the control, sample, and blank, respectively.

2.8. Statistical analysis

A two-way analysis of variance was conducted to evaluate the effects of shading levels and experimental sites. Data normality was tested using the Shapiro-Wilk test, and homogeneity of variance was assessed with the Brown-Forsythe test. Post-hoc analysis was performed using the Tukey method with a significance level of $\alpha = 0.05$. Statistical analyzes and graphical illustrations were performed using SigmaPlot 14.0 (Systat Software Inc., San Jose, CA, USA). All data met the assumption of normality; however, a few parameters did not satisfy the homogeneity of variance assumption. Consequently, the Games-Howell test was employed for post hoc comparisons using SPSS 20 (IBM Corporation, Amonk, NY, USA).

3. Results

3.1. Meteorological conditions

Rainfall variations in the forest site during the experimental period are shown in Fig. 1a. Rainfall occurred consistently throughout the year, with daily rainfall reaching 140 mm on DOE 80, 132, and 202, corresponding to approximately June, July, and October. The longest period without rainfall lasted 13 consecutive days, occurring from DOE 110 to 122 (around July). The average DLI (and relative light intensity, relative to NS within each site) during the experiment was as follows: FNS 18.85 ± 0.62 (100 %), FMS 3.94 ± 0.14 (20.9 %), FSS 1.56 ± 0.06 (8.3 %); GNS 11.87 ± 0.29 (100 %), GMS 4.28 ± 0.13 (36.1 %), GSS 1.05 ± 0.02 (8.8 %) mol photon m^{-2} day^{-1} (Fig. 1b, c). An increase in DLI was observed in FMS at the beginning and end of the experiment. The average temperature during the experimental period was 23.34 ± 0.21 °C in the forest site and 29.70 ± 0.12 °C in the greenhouse. The average relative humidity was 91.15 ± 0.36 % in the forest site and 83.93 ± 0.57 % in the greenhouse (Fig. 1d, e). Hourly light intensity variations from sunrise to sunset are presented in Fig. 2. The greenhouse exhibited a more gradual increase in light intensity throughout the day, in contrast to the forest site, which experienced more pronounced fluctuations. Notably, light intensity in FNS increased significantly between 8 a.m. and 15 pm., while in FMS, a marked increase was observed around 10 a.m. due to direct sunlight.

3.2. Growth performance

After eight months of growth, all seedlings survived under different shading conditions. Among the analyzed growth parameters, most showed significant interactions between site and shading treatments, indicating that growth responses to shading differed significantly between the forest and greenhouse environments (Table 1). For instance, root length showed no significant differences among shading treatments in the forest, whereas in the greenhouse, GMS and GSS exhibited significantly greater root lengths than GNS. Conversely, total leaf area differed significantly among shading treatments in the forest, with FMS showing the highest values, but no such differences were observed in the greenhouse. Seedling height showed no significant interaction between site and shading but was significantly reduced by shading, with the lowest height under SS. In contrast, RCD was significantly affected by both site and shading, with higher values in the greenhouse across all treatments. In the greenhouse, RCD was the highest under GMS and the lowest under GSS, while in the forest, FSS had the lowest RCD. Biomass exhibited significant interaction effects, with MS generally resulting in

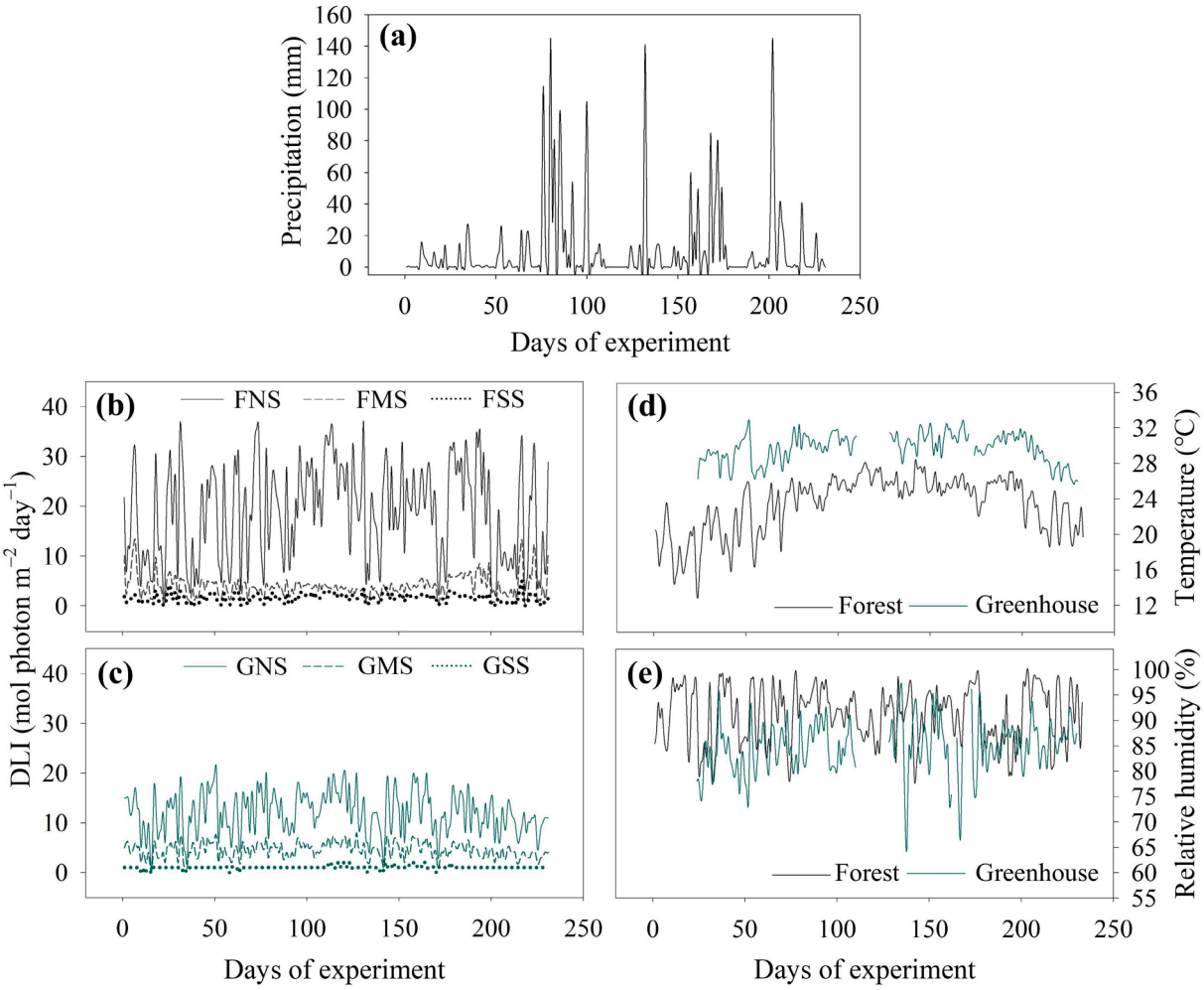

Fig. 1. Precipitation near the forest site (a); daily light integral (DLI) under three shade levels at the forest (b) and greenhouse (c); daily average temperature (d); and daily average relative humidity (e) during the experimental period. Abbreviations: F (forest), G (greenhouse), NS (no shade), MS (moderate shade), and SS (severe shade).

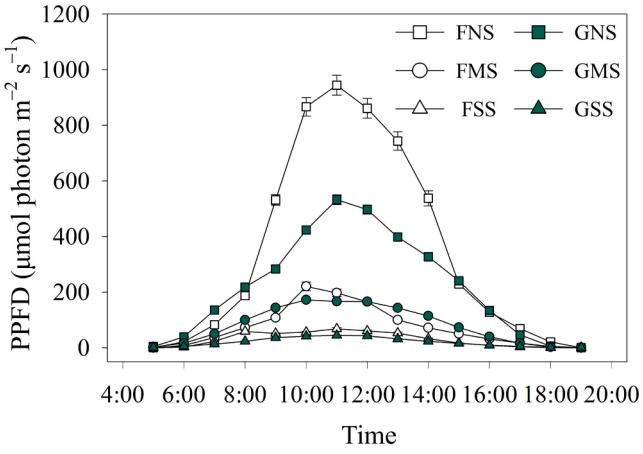

Fig. 2. Hourly photosynthetic photon flux density (PPFD) at two sites under three shade levels. Data represent the mean ± standard error during the experimental period. Abbreviations: F (forest), G (greenhouse), NS (no shade), MS (moderate shade), and SS (severe shade).

the highest values, followed by NS and SS, although these trends varied between sites. For example, root and stem biomass did not differ significantly between FNS and FMS, while leaf biomass showed no significant differences between GNS and GMS. Representative seedlings for each shading treatment are shown in Fig. S1. Seedlings under NS treatments exhibited lighter leaf coloration, with no visible damage, such as scorching or pest infestations, observed across treatments.

3.3. Photosynthetic pigments content

The chlorophyll content in leaves, including Chl *a*, Chl *b*, Cars, and Chl *a* + *b*, generally increased with higher shading levels and was consistently higher in greenhouse treatments compared to forest treatments (Table 2). Significant interactions between site and shading treatments were observed for most photosynthetic pigments. In the forest site, FMS and FSS exhibited similar pigment levels, both significantly higher than FNS. In the greenhouse, however, only GSS showed significantly higher pigment levels compared to GNS and GMS. In contrast, the Chl *a*/*b* ratio exhibited an opposite trend to photosynthetic pigment content. In the forest, FMS and FSS showed significantly lower Chl *a*/*b* ratios than FNS, while in the greenhouse, only GSS had a significantly lower ratio compared to GMS and GNS. Additionally, the Cars/Chl *a* + *b* ratio showed no significant gradient differences among greenhouse treatments, whereas in the forest, FNS had a significantly higher ratio than the other shading treatments.

Table 1
Growth response of *Ficus formosana* Maxim. at two sites under three shade levels.

Site	Shade level	RCD (mm)	Height[a] (cm)	Root length (cm)	Total leaf area (cm^2)	Root DW (g)	Stem DW (g)	Leaf DW (g)	Total DW (g)
Forest	NS	6.87a	71.35	29.76	271.47b	3.80a	6.09a	1.30b	10.39b
		(0.16)	(1.65)	(1.27)	(22.44)	(0.23)	(0.45)	(0.11)	(0.51)
	MS	6.87a	72.46	31.09	720.55a	4.26a	6.97a	2.80a	15.23a
		(0.20)	(2.08)	(1.56)	(57.57)	(0.24)	(0.51)	(0.15)	(1.04)
	SS	5.70b	68.96	27.65	352.66b	2.00b	3.48b	1.09b	6.25c
		(0.21)	(1.49)	(1.54)	(51.01)	(0.15)	(0.37)	(0.17)	(0.54)
Greenhouse	NS	8.37b*	72.72	36.14b*	770.82*	3.72b	9.15b*	3.95a*	17.31b*
		(0.31)	(1.80)	(2.45)	(46.71)	(0.38)	(0.57)	(0.34)	(1.22)
	MS	9.66a*	75.02	45.39a*	764.46	6.10a*	12.00a*	3.87a*	22.96a*
		(0.21)	(2.11)	(0.9)	(56.66)	(0.41)	(0.57)	(0.28)	(0.86)
	SS	6.67c*	67.01	45.24a*	879.42*	2.29c	4.18c	2.91b*	9.25c*
		(0.19)	(1.67)	(1.64)	(57.66)	(0.12)	(0.17)	(0.21)	(0.42)
p value	Site	**<0.001**	0.670	**<0.001**	**<0.001**	**0.004**	**<0.001**	**<0.001**	**<0.001**
	Shade	**<0.001**	**0.009**	**<0.008**	**<0.001**	**<0.001**	**<0.001**	**<0.001**	**<0.001**
	$S \times S$	**<0.001**	0.469	**<0.004**	**<0.001**	**0.003**	**<0.001**	**0.005**	**0.014**

Data represent the mean (standard error in parentheses). Different lowercase letters indicate significant differences among shade levels within the same site, while asterisks (*) denote significant differences between sites within the same shade level (two-way ANOVA, Tukey method, $\alpha = 0.05$). Sample size: RCD and seedling height ($n = 20$); other destructive measurements ($n = 10$). Abbreviations: NS (no shade), MS (moderate shade), SS (severe shade), RCD (root collar diameter), and DW (dry weight).

[a] The main effect of shade on height shows that SS is significantly lower than the other two levels.

Table 2
Leaf photosynthetic pigments content of *Ficus formosana* Maxim. at two sites under three shade levels.

Site	Shade level	Chl *a* (mg g^{-1} DW)	Chl *b* (mg g^{-1} DW)	Cars (mg g^{-1} DW)	Chl *a* + *b* (mg g^{-1} DW)	Chl *a*/*b*	Cars/Chl *a* + *b*
Forest	NS	5.38b	1.55b	1.81b	6.93b	3.53a*	0.249a*
		(0.15)	(0.06)	(0.1)	(0.21)	(0.06)	(0.002)
	MS	8.30a*	2.86a*	2.56a*	11.70a*	3.07b	0.222b*
		(0.42)	(0.18)	(0.13)	(0.65)	(0.03)	(0.001)
	SS	8.39a	2.76a	2.43a	11.15a	3.03b	0.219b
		(0.26)	(0.10)	(0.07)	(0.36)	(0.03)	(0.002)
Greenhouse	NS	7.15b*	2.23b*	2.06b	9.38b*	3.23a	0.218
		(0.09)	(0.03)	(0.04)	(0.11)	(0.03)	(0.003)
	MS	6.60b	2.17b	1.87b	8.70b	3.31a*	0.215
		(0.16)	(0.01)	(0.04)	(0.19)	(0.04)	(0.003)
	SS	11.25a*	3.79a*	3.27a*	15.04a*	2.98b	0.218
		(0.29)	(0.11)	(0.09)	(0.39)	(0.02)	(0.001)
p value	Site	**<0.001**	**<0.001**	0.708	**<0.001**	0.240	**<0.001**
	Shade	**<0.001**	**<0.001**	**<0.001**	**<0.001**	**<0.001**	**<0.001**
	$S \times S$	**<0.001**	**<0.001**	**<0.001**	**<0.001**	**<0.001**	**<0.001**

Data represent the mean (standard error in parentheses). Different lowercase letters indicate significant differences among shade levels within the same site, while asterisks (*) denote significant differences between sites within the same shade level (two-way ANOVA, Tukey method, $\alpha = 0.05$, $n = 10$). Abbreviations: NS (no shade), MS (moderate shade), SS (severe shade), Chl (chlorophyll), Cars (carotenoids), and DW (dry weight).

3.4. Morphological traits and leaf physiological responses

Among morphological parameters, the root-to-shoot ratio (R/S ratio) of dry weight was significantly higher in the forest than in the greenhouse ($p < 0.001$) (Fig. 3a). SLA and LAR both increased with shading. SLA showed no significant differences between sites, except under MS, where forest values were significantly higher than those in the greenhouse. Similarly, LAR followed the same trend under MS but was significantly higher in the greenhouse under NS and SS conditions (Fig. 3b, c). For leaf physiological responses, the Fv/Fm decreased progressively with reduced shading in the forest, whereas in the greenhouse, it increased with reduced shading (Fig. 3d). In the greenhouse, ΦPSII increased progressively with shading, while in the forest, FSS and FMS did not differ significantly, and FNS exhibited a marked decline, significantly lower than GNS (Fig. 3e). The g_s exhibited an opposite trend to ΦPSII, increasing with reduced shading in the greenhouse. In the forest, g_s was significantly higher in FNS than in FSS and FMS, and values in FNS and FSS were notably higher in the forest compared to the greenhouse (Fig. 3f). In contrast to the parameters significantly affected by site-shading interactions, RWC and MDA showed no significant interactions. Based on site effects, both RWC and MDA were significantly higher in the greenhouse than in the forest. For shading effects, RWC was higher under SS, whereas MDA was lower under SS conditions (Fig. 3g, h). Lastly, leaf H_2O_2 content in the forest was significantly elevated in FNS, reaching 4.6 times that of FSS, while no significant differences were observed among greenhouse treatments (Fig. 3i).

3.5. Leaf enzyme activities, metabolites, and antioxidant activity

The activities of antioxidant enzymes POD, APX, and CAT in *F. formosana* leaves showed no significant interaction effects between site and shading treatments (Fig. 4a–c). Among these, APX activity exhibited a significant main effect of shading ($p = 0.045$), with the highest activity under NS. Similarly, CAT activity peaked under NS and was lowest under MS, while POD activity was strongest under SS, increasing with shading intensity. Site main effects significantly influenced CAT and POD activities ($p < 0.001$), with higher overall activities

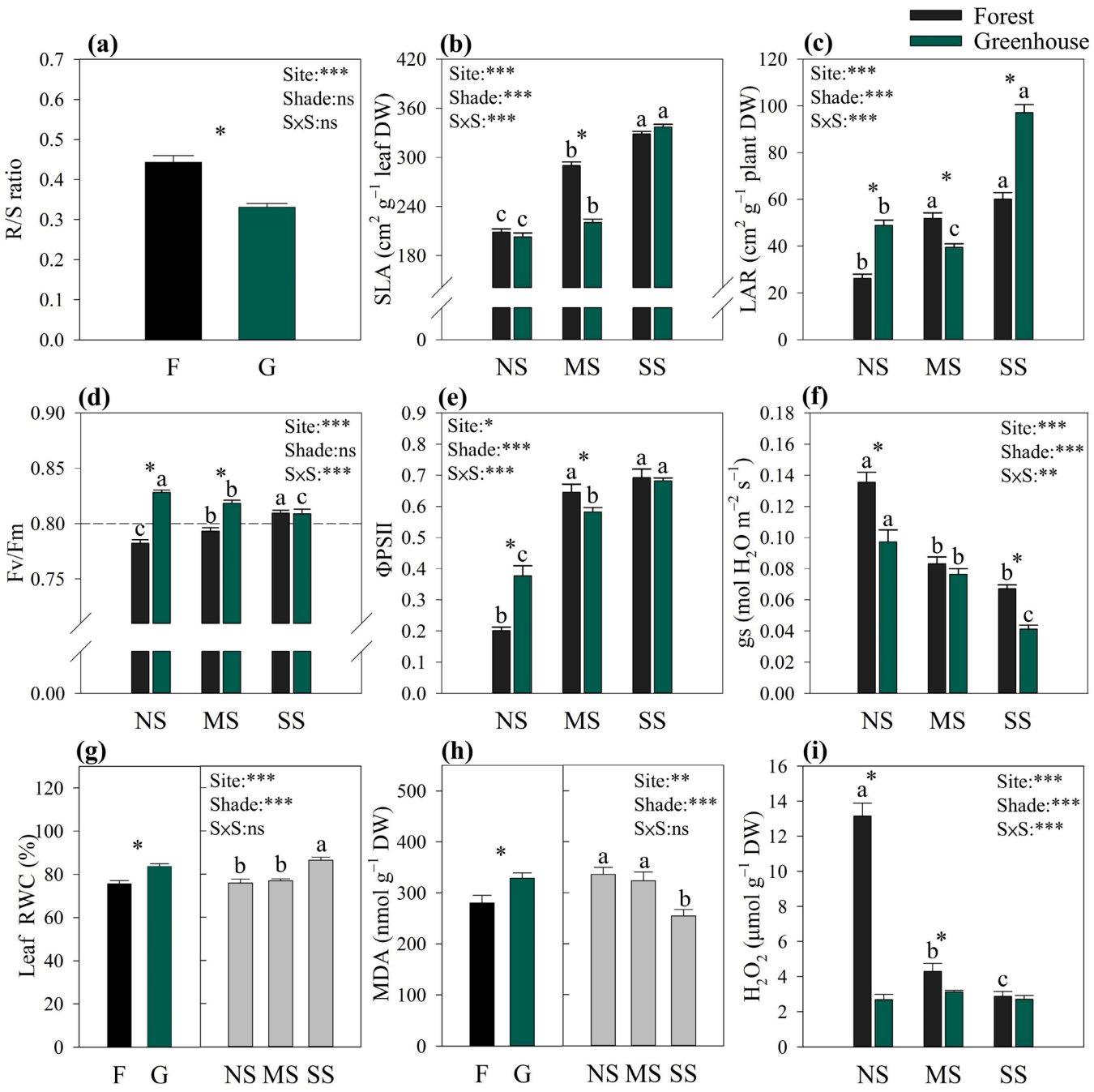

Fig. 3. Morphological traits (a–c), leaf physiological responses (d–g), and leaf oxidative stress indicators (h, i) of *Ficus formosana* Maxim. at two sites (forest and greenhouse) under three shade levels. Data represent the mean ± standard error. Two-way ANOVA results are annotated in each subplot (ns: no significance, $*p < 0.05$, $**p < 0.01$, $***p < 0.001$). Different lowercase letters indicate significant differences among shade levels or among shade levels within the same site, while asterisks (*) denote significant differences between sites or between sites within the same shade level (Tukey method, $\alpha = 0.05$, $n = 10$). Abbreviations: NS (no shade), MS (moderate shade), SS (severe shade), R/S ratio (root to shoot dry weight ratio), SLA (specific leaf area), LAR (leaf area ratio), Fv/Fm (maximum quantum efficiency of PSII), ΦPSII (quantum yield of photosystem II), g_s (stomatal conductance), RWC (relative water content), MDA (malondialdehyde), and DW (dry weight).

in forest-grown plants than in greenhouse-grown plants. For leaf primary photosynthetic metabolites, including soluble sugars, starch, and soluble proteins, were consistently higher in greenhouse plants than in forest plants and decreased significantly with increasing shading levels (Fig. 4d–f). Starch and soluble sugar contents were significantly influenced by site-shading interactions. In the greenhouse, both metabolites declined progressively from GNS to GSS, whereas in the forest, FNS exhibited the highest contents, with levels decreasing under FMS and stabilizing at FSS. For leaf secondary metabolites, including TPC and TFC, significant interactions between site and shading treatments were observed (Fig. 4g, h). In the forest, TPC and TFC were highest under FNS. In the greenhouse, TPC was highest under GMS, while TFC increased progressively with shading intensity. DPPH-RSA followed a similar trend to TPC, with the highest activity in FNS in the forest and GMS in the greenhouse (Fig. 4i).

3.6. Root metabolites and antioxidant activity

The soluble sugar content in the roots of *F. formosana* exhibited a trend similar to that in the leaves, with significantly higher levels in FNS

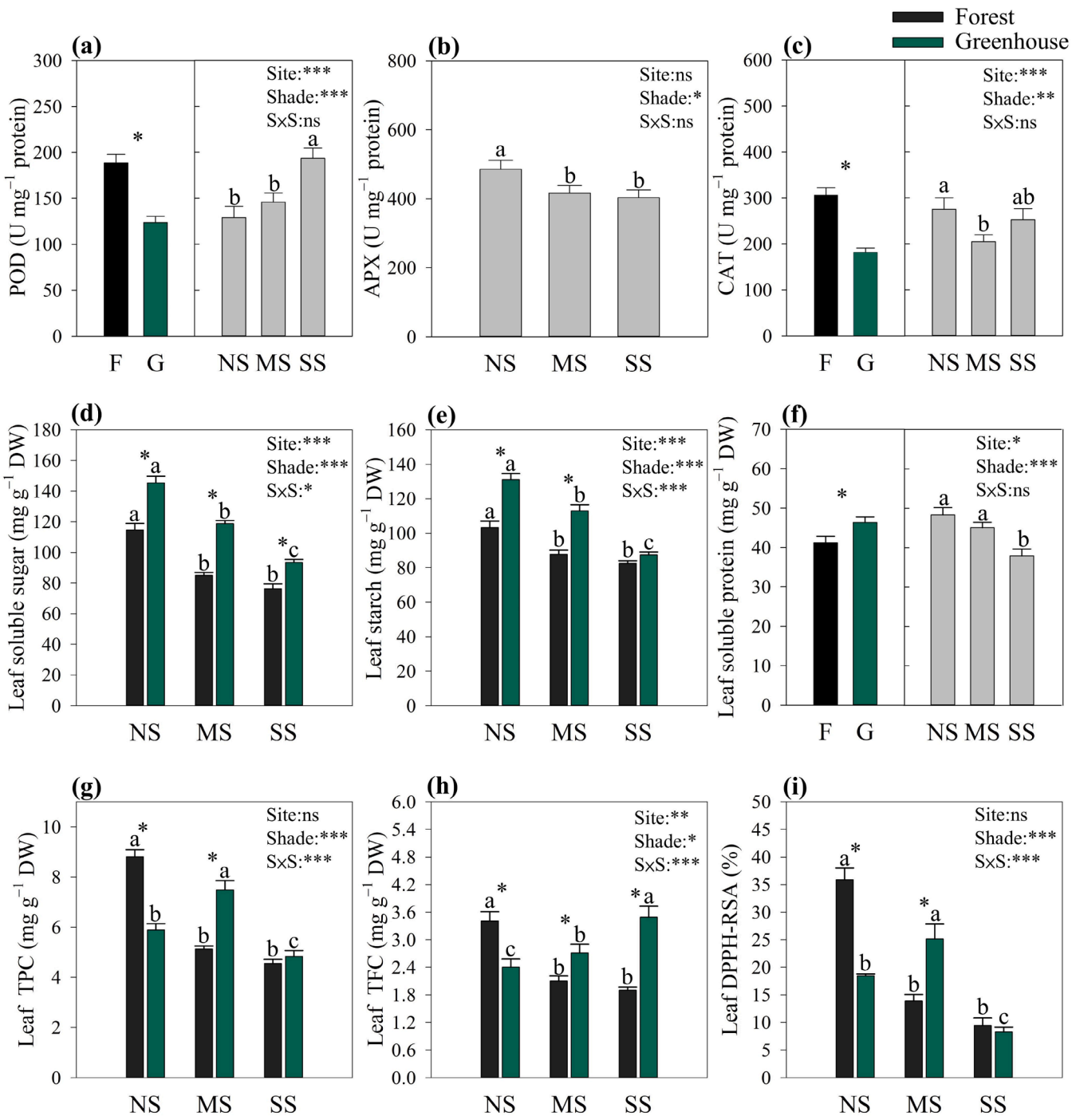

Fig. 4. Leaf enzyme activities (a–c), metabolites (d–h), and antioxidant activity (i) of *Ficus formosana* Maxim. at two sites (forest and greenhouse) under three shade levels. Data represent the mean ± standard error. Two-way ANOVA results are annotated in each subplot (ns: no significance, *$p < 0.05$, **$p < 0.01$, ***$p < 0.001$). Different lowercase letters indicate significant differences among shade levels or among shade levels within the same site, while asterisks (*) denote significant differences between sites or between sites within the same shade level (Tukey method, $\alpha = 0.05$, $n = 10$). Abbreviations: NS (no shade), MS (moderate shade), SS (severe shade), POD (peroxidase), APX (ascorbate peroxidase), CAT (catalase), TPC (total phenolic compounds), TFC (total flavonoids compounds), DPPH-RSA (DPPH radicals scavenging ability), and DW (dry weight).

compared to FMS and FSS in the forest, but no significant differences among shading treatments in the greenhouse (Fig. 5a). Similarly, root starch content was significantly higher in FNS in the forest, whereas in the greenhouse, GMS showed significantly higher levels than GSS (Fig. 5b). For root TPC, no significant differences were observed among shading treatments in the forest, while in the greenhouse, both GSS and GMS had significantly higher levels than GNS (Fig. 5c). In contrast, root TFC followed an opposite trend, with the highest levels in FNS in the forest, but higher levels in GSS in the greenhouse (Fig. 5d). Finally, root DPPH-RSA was significantly influenced by the main effect of site, with higher values in the greenhouse compared to the forest ($p = 0.002$) (Fig. 5e).

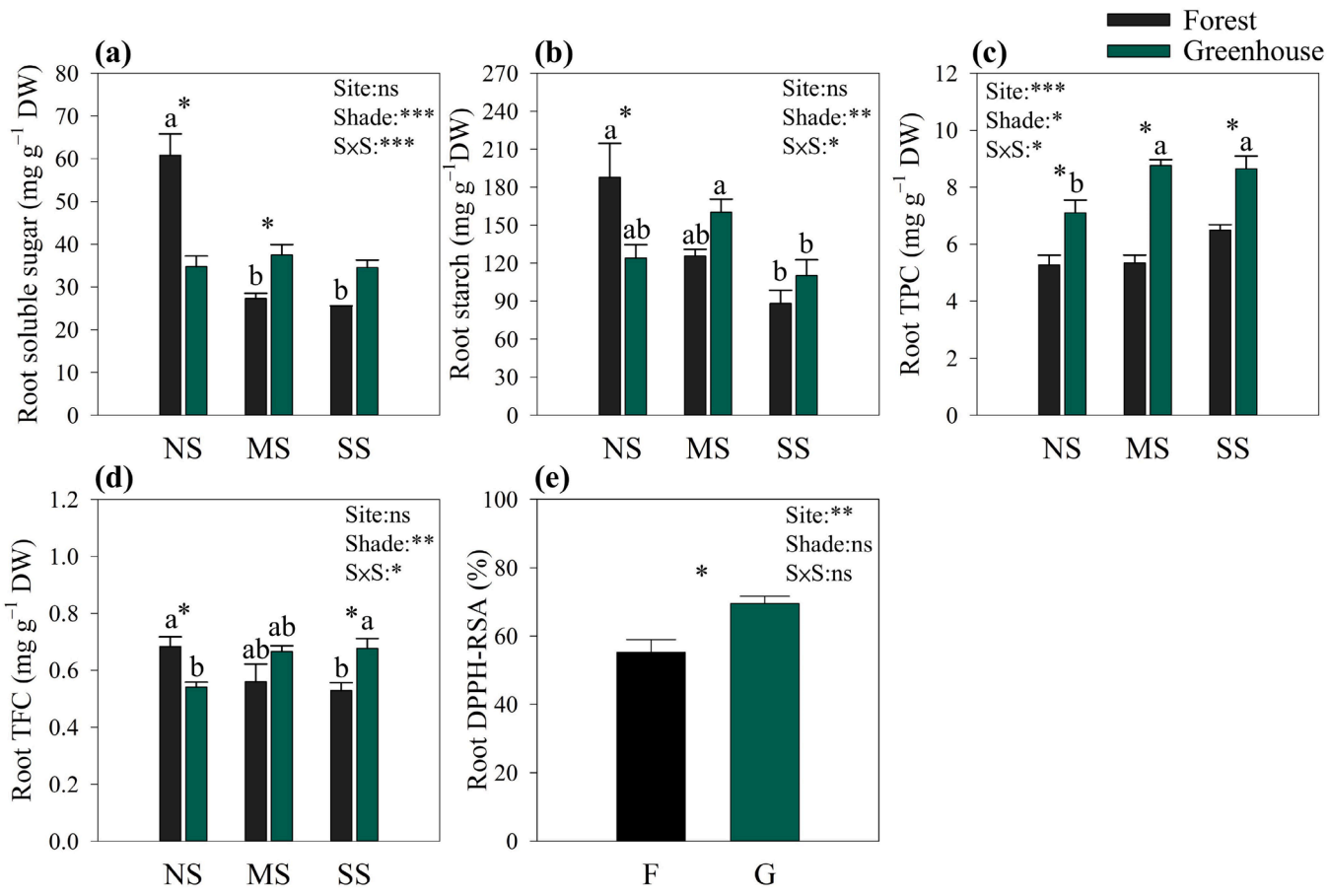

Fig. 5. Root metabolites (a–d) and antioxidant activity (e) of *Ficus formosana* Maxim. at two sites (forest and greenhouse) under three shade levels. Data represent the mean ± standard error. Two-way ANOVA results are annotated in each subplot (ns: no significance, $^{*}p < 0.05$, $^{**}p < 0.01$, $^{***}p < 0.001$). Different lowercase letters indicate significant differences among shade levels within the same site, while asterisks (*) denote significant differences between sites or between sites within the same shade level (Tukey method, $\alpha = 0.05$, $n = 10$). Abbreviations: NS (no shade), MS (moderate shade), SS (severe shade), TPC (total phenolic compounds), TFC (total flavonoids compounds), DPPH-RSA (DPPH radicals scavenging ability), and DW (dry weight).

4. Discussion

4.1. Effects of different shades on growth and physiological performance

Plant biomass reflects the net balance between photosynthesis and respiration under varying environmental conditions, serving as a direct indicator of growth performance. After eight months of growth, *F. formosana* exhibited the highest total dry weight under MS conditions, with growth reduced under NS and SS treatments. The most pronounced suppression occurred under SS, highlighting the species' preference for moderate light availability (DLI ~4 mol photon m^{-2} day^{-1}), consistent with its classification as a moderately shade-tolerant species (Kuo et al., 2021). In the forest, the intense light under FNS significantly inhibited leaf growth. Similarly, in the greenhouse, despite the shading provided by the plastic covering, GNS light intensity likely exceeded the species' tolerance range, reducing root and stem biomass. ΦPSII measurements prior to sampling revealed that NS treatments at both sites had relatively low values, with the greatest decline observed under FNS, the highest light intensity treatment. This suggests that prolonged excessive light exposure caused photoinhibition, impairing PSII activity and biomass accumulation (Hussain et al., 2020). Morphological parameters further elucidated the light adaptation strategies of *F. formosana*, supporting its ability to adjust to both high- and low-light environments by optimizing carbon gain and resource allocation (Givnish, 1988; Valladares et al., 2016). Under NS conditions, SLA decreased significantly, resulting in thicker, smaller leaves with well-developed palisade tissues—an adaptation that enhances water retention and light-use efficiency under high light conditions (Wyka et al., 2012; Poorter et al., 2019). Conversely, under SS conditions at both sites, SLA and LAR were significantly elevated, reflecting shade-adaptive strategies that prioritize resource allocation to leaf expansion, producing larger, thinner leaves to enhance light capture (Poorter et al., 2009).

Under NS conditions at both sites, ΦPSII and photosynthetic pigment content decreased, reflecting an adaptive strategy to reduce light absorption and mitigate photodamage (Alter et al., 2012). In parallel, g_s significantly increased, enhancing transpiration and heat dissipation under intense light exposure (Poorter et al., 2019). Strong UV radiation under FNS further induced TPC and TFC accumulation, which scavenge ROS and absorb high-energy UV radiation (de Araújo et al., 2017). The increased Cars/Chl $a + b$ ratio indicated an enhanced xanthophyll cycle activity, dissipating excess light energy as heat and reducing oxidative damage (Telfer, 2014). Additionally, high CAT activity efficiently scavenged H_2O_2 from photorespiration, while APX activity addressed H_2O_2 accumulation in chloroplasts via the AsA-GSH cycle (Willekens et al., 1997; Bao et al., 2021; Bechtold et al., 2008). In contrast, POD activity significantly increased with higher shading levels, reflecting the ability of *F. formosana* to effectively regulate various antioxidant enzymes to scavenge ROS generated under different light stress conditions, thereby maintaining oxidative balance in the leaves (Wang et al., 2021). Nevertheless, substantial H_2O_2 accumulation was observed in FNS leaves, indicating that under strong light exposure, photon absorption exceeded the capacity of carbon reactions for utilization, resulting in excessive ROS production that could not be effectively mitigated by antioxidant mechanisms (Foyer, 2018). This was accompanied by

reduced photosynthetic pigment content, lower Fv/Fm values, and elevated MDA levels, marking oxidative damage to PSII and the light-harvesting complex (Cifuentes and Moreno, 2022). In comparison, GNS experienced milder oxidative stress due to reduced light intensity provided by the translucent greenhouse covering.

Under SS conditions at both sites, low H_2O_2 and MDA levels were observed, along with increased ΦPSII and photosynthetic pigment content, suggesting that oxidative stress was not a limiting factor for growth (Contin et al., 2014). Instead, reduced g_s indicated stomatal limitations, which restricted CO_2 diffusion into leaves, ultimately reducing photosynthetic carbon assimilation and biomass accumulation. To adapt to limited light availability, plants expanded their leaf area to maximize light capture, but this came at a cost: as leaf area increased, stomatal density declined, leading to reduced stomatal conductance, which constrained CO_2 uptake, while reducing transpiration also helped maintain water balance under shaded conditions (Ajmi et al., 2018). Notably, when comparing FNS and FSS, leaf dry weight remained unchanged, while stem and root biomass declined significantly, indicating a shift in resource allocation toward leaf expansion under severe shading. This shift highlights a fundamental trade-off: while larger leaves enhance light capture, the overall low light availability still constrains carbon gain, limiting resource allocation to stems and roots. As a result, despite morphological adjustments to maximize light capture, prolonged severe shading ultimately restricts photosynthetic efficiency and biomass accumulation, posing significant challenges to plant growth and physiological balance.

4.2. Discrepancies in adaptive strategies between greenhouse and forest environments

Photosynthetic pigments, such as Chl *a*, Chl *b*, and Cars, are key molecules for capturing light energy, and their quantification provides critical insights into the photosynthetic status of plants (Simkin et al., 2022). In *F. formosana* grown in two environments, chlorophyll and Cars contents generally increased under shaded conditions, aligning with the observation that shade-tolerant plants enhance chloroplast density to optimize light capture under low-light availability (Esteban et al., 2015). Beyond light intensity, light quality also played a crucial role in pigment regulation, as spectral differences between the forest and greenhouse environments influenced pigment composition and function. In forests, canopy absorption of red light increases the blue/red light ratio while decreasing the red/far-red ratio, thereby modifying the spectral composition of light (Goldstein et al., 2016; Navrátil et al., 2007). Under these conditions, shade-tolerant species primarily adopt physiological adjustments, including increased levels of accessory pigments such as Chl *b* and Cars to optimize light harvesting, as well as higher SLA or LAR to improve light capture, whereas species employing a shade-avoidance strategy respond to shading with stem elongation (Gommers et al., 2013; Osunkoya et al., 1994). In line with shade-tolerant strategies, *F. formosana* exhibited these patterns under forest shade conditions in this study. Conversely, in the greenhouse, where artificial black shading nets primarily reduced light intensity without significantly altering the spectral distribution of red, blue, or far-red light (Kotilainen et al., 2018; Rodríguez-López et al., 2014), substantial changes in pigment content and leaf morphological parameters were observed only under severe shading. These responses were more closely associated with excessively low light intensity rather than spectral modifications. Collectively, these findings suggest that *F. formosana* adapts to low-light environments through coordinated adjustments in photosynthetic pigments, leaf morphology, and biomass allocation. Furthermore, the dynamic light conditions in the forest, characterized by sunflecks and spectral shifts, play a crucial role in regulating pigments and leaf morphology—an aspect that greenhouse experiments fail to fully replicate.

F. formosana exhibited distinct carbohydrate allocation patterns between greenhouse and forest environments, primarily driven by differences in water availability and light intensity. In both environments, leaf soluble sugar and starch contents decreased with increasing shade, reflecting reduced carbon assimilation under lower light availability (Martins et al., 2014; Li et al., 2016). However, root carbohydrate responses diverged significantly. In the forest, drought stress in FNS induced a substantial increase in root soluble sugar levels, lowering root water potential to enhance water uptake (Du et al., 2020). In contrast, the greenhouse provided a stable water supply, resulting in no significant variation in root soluble sugar content across shading treatments. Additionally, stable water availability increased leaf RWC, which promoted aboveground tissue development (Coutand et al., 2008). The higher R/S ratio in the forest compared to the greenhouse further suggests that under limited water availability, *F. formosana* prioritizes root biomass accumulation to enhance water acquisition and improve resilience against environmental stress. Starch partitioning also differed between environments. In the forest, root starch content decreased with shade, mirroring leaf carbohydrate trends. However, in the greenhouse, root starch accumulation peaked under moderate shading. This pattern suggests that in a controlled environment with stable resources, moderate shading optimized carbon translocation from leaves to roots, improving CO_2 assimilation efficiency (Thitisaksakul et al., 2017). Additionally, starch granules sedimented in root tips due to gravity, promoting root elongation (Baldwin et al., 2013). Conversely, in the forest, strong light stress in FNS likely triggered increased root carbon storage as a protective strategy against environmental fluctuations. These discrepancies highlight the influence of environmental stability on carbohydrate partitioning. Under greenhouse conditions, carbon allocation prioritizes active growth due to stable water and shading conditions, whereas in the forest, stronger light stress and limited water availability favor a conservative strategy of belowground carbon storage for long-term survival.

4.3. Antioxidant capacity in response to shading conditions

The primary human use of *F. formosana* lies in its roots, which are widely consumed for dietary and medicinal purposes due to their rich bioactive compounds, particularly phenolic compounds such as flavonoids. These compounds provide antioxidant, anti-inflammatory, and anti-tumor benefits (Huang et al., 2013) and enhance plant stress tolerance by mitigating oxidative damage, chelating reactive metal ions, and preventing lipid peroxidation (Naikoo et al., 2019). In this study, root TPC and TFC increased with shading levels under greenhouse conditions. In low-light environments, where carbon sources are limited, plants may prioritize secondary metabolite accumulation over growth to enhance stress tolerance (Hou et al., 2010). Flavonoids, a key group of phenolic compounds, are particularly effective in photoprotection, especially against UV-B radiation (Csepregi et al., 2018). In the forest, the higher UV exposure in FNS likely induced TFC accumulation in leaves, which may have been transported to roots to support overall defense mechanisms. DPPH-RSA, a measure of radical scavenging activity, reflects the antioxidant capacity of plant tissues and is influenced by phenolic compounds, antioxidant enzymes, carotenoids, and other bioactive substances (Ibrahim et al., 2011; Xu et al., 2012; Gan et al., 2017). The similar trends observed between leaf TPC and DPPH-RSA across light conditions suggest that phenolic compounds predominantly drive the antioxidant capacity of leaf extracts. In roots, DPPH-RSA was higher in greenhouse samples than in the forest, likely due to elevated TPC levels. However, shading did not significantly affect root DPPH-RSA, indicating that the antioxidant quality of *F. formosana* roots remained stable under different light conditions. Notably, an increase in plant biomass can lead to a reduction in biochemical compound concentrations, a phenomenon known as the dilution effect (Génard et al., 2014). However, in this study, moderate shading not only enhanced root biomass but also maintained the health benefits of bioactive compounds, showing no dilution effect on antioxidant capacity (Qaderi et al., 2023). This suggests that higher root yields can be achieved without compromising functional value.

4.4. Implications for sustainable under-forest cultivation

Taiwan promotes under-forest economy policies partly due to the long growth cycle of trees and its geographical location in the northwestern Pacific, making it highly susceptible to typhoons, which lead to uncertainties in timber revenues. The development of the NTFPs industry has generated both ecological and economic benefits, contributing to forest conservation while enhancing farmers' incomes (Dou et al., 2023). In this study, one-year-old *F. formosana* seedlings were used for a monitoring experiment lasting approximately one year. According to Forestry and Nature Conservation Agency (FANCA) (2023), *F. formosana* can be harvested after two years of growth in forested areas, providing rapid economic returns for forest farmers. The short-term experimental results of this study provide valuable insights for forest farmers in cultivation practices. Currently, the applications of *F. formosana* extend beyond its commonly used roots and stems for soup preparation; its leaves are also processed into tea, allowing full utilization of the plant (Chen et al., 2022). The results of this study indicate that moderate shading promotes seedling growth and significantly enhances leaf biomass accumulation. Therefore, forest farmers can select sites with moderate canopy closure for cultivation to maximize yield. Additionally, the choice of shade tree species is a critical factor, as mixed-species planting can enhance ecological resilience and reduce the risk of monoculture pest outbreaks (Jactel et al., 2021). Since different tree species exhibit different light transmittance properties, an appropriately mixed planting strategy can regulate light conditions in forested areas, providing a favorable growth environment for *F. formosana*. Furthermore, the increasing frequency of drought and extreme heat events due to climate change has led to significant declines in crop yields. For instance, as the world's largest producer of Arabica coffee, Brazil's growing regions are persistent climate change hotspots, where extreme weather is expected to reduce yields (Dias et al., 2024). Agroforestry has been shown to mitigate the impact of extreme climate events and sustain areas suitable for coffee cultivation (Gomes et al., 2020). Taiwan's under-forest economy approach prioritizes tree growth while incorporating short-term understory crops, which are limited to native species, balancing ecological and economic considerations. In this study, although greenhouse temperatures were relatively high, no significant heat damage was observed, and the seedlings grew well under moderate shading. Moreover, *F. formosana* demonstrated the ability to adjust its morphological and physiological traits in response to varying light environments in forest ecosystems, enhancing its adaptability to different understory conditions. These findings suggest that *F. formosana*'s tolerance to both high temperatures and shade may offer a cultivation advantage, contributing to the sustainability of agroforestry systems under climate change.

5. Conclusion

This study examined the growth performance, physiological adaptations, and biochemical accumulation of *F. formosana* under different shading environments. Our results indicate that moderate shading promotes optimal biomass accumulation, demonstrating its suitability for under-forest cultivation. In the greenhouse, *F. formosana* grew well with relatively stable light and irrigation, showing significant growth inhibition only under severe shading, which induced pigment accumulation and leaf morphological changes. In contrast, unshaded forest conditions caused oxidative stress, leading to increased antioxidant enzyme activity and enhanced root sugar accumulation for water uptake. Under shaded forest conditions, higher photosynthetic pigment content, SLA, and LAR were observed, likely due to sunflecks and changes in light quality beneath the canopy. These findings suggest that *F. formosana* exhibits typical shade-tolerant traits, adapting to low-light environments through physiological and morphological adjustments. Additionally, moderate shading maintained stable levels of secondary metabolites and antioxidant capacity in the roots, ensuring both yield and functional quality. These findings reinforce the potential of *F. formosana* as a sustainable under-forest crop and provide insights for optimizing its cultivation.

CRediT authorship contribution statement

Ping-Huan Tsai: Methodology, Investigation. **Yao-Yu Chiang:** Writing – review & editing, Investigation. **Chih-Ming Lai:** Writing – review & editing, Project administration. **Hung-Chih Lin:** Writing – review & editing, Resources. **Yao-Moan Huang:** Writing – review & editing, Resources. **Tzu-Hao Su:** Writing – original draft, Visualization, Methodology, Investigation, Formal analysis, Conceptualization.

Declaration of competing interest

The authors declare that they have no known competing financial interests or personal relationships that could have appeared to influence the work reported in this paper.

Acknowledgments

The authors thank Shin-Der Lin, Yuan-Shiang Lin, Jei-Chen Wu, Jiun-Tze Chang, Wei-Cheng, Song, and Jian-Wen, Gao for their assistance in field investigations.

Supplementary materials

Supplementary material associated with this article can be found, in the online version, at doi:10.1016/j.tfp.2025.100853.

Data availability

Data will be made available on request.

References

Abbasi Surki, A., Nazari, M., Fallah, S., Iranipour, R., Mousavi, A., 2020. The competitive effect of almond trees on light and nutrients absorption, crop growth rate, and the yield in almond–cereal agroforestry systems in semi-arid regions. Agrofor. Syst. 94 (3), 1111–1122.

Aebi, H., 1984. Catalase in vitro. Meth. Enzym. 105, 121–126.

Ajmi, A., Vázquez, S., Morales, F., Chaari, A., El-Jendoubi, H., Abadía, A., Larbi, A., 2018. Prolonged artificial shade affects morphological, anatomical, biochemical and ecophysiological behavior of young olive trees (cv. Arbosana). Sci. Hortic. 241, 275–284.

Alexieva, V., Sergiev, I., Mapelli, S., Karanov, E., 2001. The effect of drought and ultraviolet radiation on growth and stress markers in pea and wheat. Plant Cell Env. 24 (12), 1337–1344. https://doi.org/10.1046/j.1365-3040.2001.00778.x.

Alter, P., Dreissen, A., Luo, F.L., Matsubara, S., 2012. Acclimatory responses of *Arabidopsis* to fluctuating light environment: comparison of different sunfleck regimes and accessions. Photosyn. Res. 113 (1), 221–237.

Baldwin, K.L., Strohm, A.K., Masson, P.H., 2013. Gravity sensing and signal transduction in vascular plant primary roots. Am. J. Bot. 100 (1), 126–142.

Bao, H., Morency, M., Rianti, W., Saeheng, S., Roje, S., Weber, A.P., Walker, B.J., 2021. Catalase protects against nonenzymatic decarboxylations during photorespiration in *Arabidopsis thaliana*. Plant Direct. 5 (12), e366. https://doi.org/10.1002/pld3.366.

Bechtold, U., Richard, O., Zamboni, A., Gapper, C., Geisler, M., Pogson, B., Karpinski, S., Mullineaux, P.M., 2008. Impact of chloroplastic- and extracellular-sourced ROS on high light-responsive gene expression in *Arabidopsis*. J. Exp. Bot. 59 (2), 121–133.

Bradford, M.M., 1976. A rapid and sensitive method for the quantitation of microgram quantities of protein utilizing the principle of protein-dye binding. Anal. Biochem. 72 (1–2), 248–254.

Brand-Williams, W., Cuvelier, M.E., Berset, C., 1995. Use of a free radical method to evaluate antioxidant activity. LWT-Food Sci. Technol. 28 (1), 25–30.

Chamberlain, J.L., Mitchell, D., Brigham, T., Hobby, T., Zabek, L., Davis, J., 2009. Forest farming practices. editor. In: Gene Garrett, H.E. (Ed.), North American Agroforestry: An Integrated Science and Practice, 2nd ed. American Society of Agronomy, Madison, WI, USA, pp. 219–256.

Chance, B., Maehly, A., 1955. Assay of catalases and peroxidases. Methods Enzym. 2, 764–775.

Chang, C.C., Yang, M.H., Wen, H.M., Chern, J.C., 2002. Estimation of total flavonoid content in propolis by two complementary colorimetric methods. J. Food Drug Anal. 10, 178–182. https://doi.org/10.38212/2224-6614.2748.

Chen, F.C., 2022. The origin and promotion of understory economy in Taiwan. For. Res. Newsl. 29 (1), 23–27 [in Chinese]. https://www.airitilibrary.com/Article/Detail?DocID=16056922-202202-202205040014-202205040014-23-27.
Chen, G.W., Chen, T.Y., Yang, P.M., 2022. Differential effect of herbal tea extracts on free fatty acids-, ethanol- and acetaminophen-induced hepatotoxicity in FL83B hepatocytes. Drug Chem. Toxicol. 45 (1), 347–352.
Cifuentes, L., Moreno, F., 2022. Trait coordination at leaf level explains the resistance to excess light stress in shade-tolerant tropical tree species. Tree Physiol. 42 (7), 1325–1336.
Contin, D.R., Soriani, H.H., Hernández, I., Furriel, R.P.M., Munné-Bosch, S., Martinez, C. A., 2014. Antioxidant and photoprotective defenses in response to gradual water stress under low and high irradiance in two Malvaceae tree species used for tropical forest restoration. Trees 28 (6), 1705–1722.
Coutand, C., Dupraz, C., Jaouen, G., Ploquin, S., Adam, B., 2008. Mechanical stimuli regulate the allocation of biomass in trees: demonstration with young *Prunus avium* trees. Ann. Bot. 101 (9), 1421–1432.
Csepregi, K., Hideg, É., 2018. Phenolic compound diversity explored in the context of photo-oxidative stress protection. Phytochem. Anal. 29 (2), 129–136.
De Almeida, J., Herrera, A., Tezara, W., 2019. Phenotypic plasticity to photon flux density of physiological, anatomical and growth traits in a modern Criollo cocoa clone. Physiol. Plant 166 (3), 821–832.
de Araújo, R.P., de Almeida, A.A.F., Barroso, J.P., de Oliveira, R.A., Gomes, F.P., Ahnert, D., Baligar, V., 2017. Molecular and morphophysiological responses cocoa leaves with different concentrations of anthocyanin to variations in light levels. Sci. Hortic. 224, 188–197.
Deng, B.O., Shang, X., Fang, S., Li, Q., Fu, X., Su, J., 2012. Integrated effects of light intensity and fertilization on growth and flavonoid accumulation in *Cyclocarya paliurus*. J. Agric. Food Chem. 60 (25), 6286–6292.
Dias, C.G., Martins, F.B., Martins, M.A., 2024. Climate risks and vulnerabilities of the Arabica coffee in Brazil under current and future climates considering new CMIP6 models. Sci. Total Environ. 907, 167753. https://doi.org/10.1016/j.scitotenv.2023.167753.
Dou, Y., Wu, J., Li, Y., Chen, X., Zhao, X., 2023. Has the development of the non-timber forest products industry achieved poverty alleviation? Evidence from lower-income forest areas in Yunnan Province. Forests. 14 (4), 776.
Du, Y., Zhao, Q., Chen, L., Yao, X., Zhang, W., Zhang, B., Xie, F., 2020. Effect of drought stress on sugar metabolism in leaves and roots of soybean seedlings. Plant Physiol. Biochem. 146, 1–12.
DuBois, M., Gilles, K.A., Hamilton, J.K., Rebers, P.A., Smith, F., 1956. Colorimetric method for determination of sugars and related substances. Anal. Chem. 28 (3), 350–356.
Esteban, R., Barrutia, O., Artetxe, U., Fernández-Marín, B., Hernández, A., García-Plazaola, J.I., 2015. Internal and external factors affecting photosynthetic pigment composition in plants: a meta-analytical approach. New Phytol. 206 (1), 268–280.
Esterbauer, H., Cheeseman, K.H., 1990. Determination of aldehydic lipid peroxidation products: malonaldehyde and 4-hydroxynonenal. Methods Enzym. 186, 407–421.
Feng, J., Zhao, K., He, D., Fang, S., Lee, T., Chu, C., He, F., 2018. Comparing shade tolerance measures of woody forest species. PeerJ. 6, e5736.
Firmino, T.P., de Souza, L.A., Barbeiro, C., Marcílio, T., Romagnolo, M.B., Pastorini, L.H., 2021. Influence of the light on the morphophysiological responses of native trees species of the semidecidual stational forest. Braz. J. Bot. 44 (4), 963–976.
Forestry and Nature Conservation Agency (FANCA), 2023. Technical guidelines for under-forest economy. FANCA. https://www.forest.gov.tw/file.aspx?fno=86922 (accessed 1 March 2025).
Foyer, C.H., 2018. Reactive oxygen species, oxidative signaling and the regulation of photosynthesis. Env. Exp. Bot. 154, 134–142.
Gan, J., Feng, Y., He, Z., Li, X., Zhang, H., 2017. Correlations between antioxidant activity and alkaloids and phenols of maca (*Lepidium meyenii*). J. Food Qual. 2017 (1), 3185945. https://doi.org/10.1155/2017/3185945.
Garcia-Caparros, P., De Filippis, L., Gul, A., Hasanuzzaman, M., Ozturk, M., Altay, V., Lao, M.T., 2021. Oxidative stress and antioxidant metabolism under adverse environmental conditions: a review. Bot. Rev. 87, 421–466.
García-Pérez, J.L., Oliet, J.A., Villar-Salvador, P., Guzmán, J.E., 2021. Root growth dynamics and structure in seedlings of four shade tolerant mediterranean species grown under moderate and low light. Forests. 12 (11), 1540.
Génard, M., Baldazzi, V., Gibon, Y., 2014. Metabolic studies in plant organs: don't forget dilution by growth. Front. Plant Sci. 5, 85. https://doi.org/10.3389/fpls.2014.00085.
Givnish, T.J., 1988. Adaptation to sun and shade: a whole-plant perspective. Funct. Plant Biol. 15 (2), 63–92. https://doi.org/10.1071/PP9880063.
Goldstein, G., Santiago, L.S., Campanello, P.I., Avalos, G., Zhang, YJ., Villagra, M., 2016. In: Goldstein, G., Santiago, L. (Eds.), Tropical Tree Physiology. Tree Physiology, 6. Springer, Cham. https://doi.org/10.1007/978-3-319-27422-5_15.
Gomes, L.C., Bianchi, F.J.J.A., Cardoso, I.M., Fernandes, R.B.A., Fernandes Filho, E.I., Schulte, R.P.O, 2020. Agroforestry systems can mitigate the impacts of climate change on coffee production: a spatially explicit assessment in Brazil. Agric. Ecosyst. Env. 294, 106858.
Gommers, C.M., Visser, E.J., St Onge, K.R., Voesenek, L.A., Pierik, R., 2013. Shade tolerance: when growing tall is not an option. Trends. Plant Sci. 18 (2), 65–71.
Hou, J.L., Li, W.D., Zheng, Q.Y., Wang, W.Q., Xiao, B., Xing, D., 2010. Effect of low light intensity on growth and accumulation of secondary metabolites in roots of *Glycyrrhiza uralensis* Fisch. Biochem. Syst. Ecol. 38 (2), 160–168.
Huang, Y.H., 2018. Exploring Taiwan's unique under-forest economy through agroforestry. For. Res. Newsl. 25 (1), 1–4 [in Chinese]. https://www.airitilibrary.com/Article/Detail?DocID=16056922-201802-201803270006-201803270006-1-4.
Huang, G.J., Deng, J.S., Huang, S.S., Wang, S.Y., Chang, Y.S., Kuo, Y.H., 2013. Bioassay guided isolation and identification of anti-inflammatory active compounds from the root of *Ficus formosana*. J. Agric. Food Chem. 61 (46), 11008–11015.
Hussain, M.I., Tsombou, F.M., El-Keblawy, A., 2020. Surface canopy position determines the photosystem II photochemistry in invasive and native *Prosopis* congeners at Sharjah Desert. UAE. For. 11 (7), 740.
Ibrahim, M.H., Jaafar, H.Z., Rahmat, A., Rahman, Z.A., 2011. Involvement of nitrogen on flavonoids, glutathione, anthocyanin, ascorbic acid and antioxidant activities of Malaysian medicinal plant *Labisia pumila* Blume (Kacip Fatimah). Int. J. Mol. Sci. 13 (1), 393–408.
Jactel, H., Moreira, X., Castagneyrol, B., 2021. Tree diversity and forest resistance to insect pests: patterns, mechanisms, and prospects. Annu. Rev. Entomol. 66 (1), 277–296.
Jung, M.J., Yang, C.K., 2002. An Ethnobotanical Memory of Taiwan. Morning Star Publishing Inc, Taichung City, Taiwan, p. 195 [in Chinese].
Kang, H., Tomimatsu, H., Zhu, T., Ma, Y., Wang, X., Zhang, Y., Tang, Y., 2022. Contributions of species shade tolerance and individual light environment to photosynthetic induction in tropical tree seedlings. Tree Physiol. 42 (10), 1975–1987. https://doi.org/10.1093/treephys/tpac056.
Kotilainen, T., Robson, T.M., Hernandez, R., 2018. Light quality characterization under climate screens and shade nets for controlled-environment agriculture. PLoS. One 13 (6), e0199628.
Krause, G.H., Winter, K., Matsubara, S., Krause, B., Jahns, P., Virgo, A., García, M., 2012. Photosynthesis, photoprotection, and growth of shade-tolerant tropical tree seedlings under full sunlight. Photosyn. Res. 113, 273–285.
Kuo, Y.L., Lin, T.Y., Yang, Y.Y., Chen, H.L., Yang, C.K., Yu, S.Y., 2021. Photosynthetic characteristics and shade tolerance of 440 native woody species in Taiwan. Taiwan J. For. Sci. 36 (3), 189–220. https://doi.org/10.7075/TJFS.202109_36(3).0002 [in Chinese with English summary].
Li, N., He, N., Yu, G., Wang, Q., Sun, J., 2016. Leaf non-structural carbohydrates regulated by plant functional groups and climate: evidences from a tropical to cold-temperate forest transect. Ecol. Indic. 62, 22–31.
Lichtenthaler, H.K., 1987. Chlorophylls and carotenoids: pigments of photosynthetic biomembranes. Meth. Enzym. 148, 350–382.
Martins, S.C.V., Araújo, W.L., Tohge, T., Fernie, A.R., DaMatta, F.M., 2014. In high-light-acclimated coffee plants the metabolic machinery is adjusted to avoid oxidative stress rather than to benefit from extra light enhancement in photosynthetic yield. PLoS. One 9 (4), e94862.
Mathur, S., Jain, L., Jajoo, A., 2018. Photosynthetic efficiency in sun and shade plants. Photosynthetica 56, 354–365.
Morales, L.O., Tegelberg, R., Brosché, M., Keinänen, M., Lindfors, A., Aphalo, P.J., 2010. Effects of solar UV-A and UV-B radiation on gene expression and phenolic accumulation in *Betula pendula* leaves. Tree Physiol. 30 (7), 923–934.
Naikoo, M.I., Dar, M.I., Raghib, F., Jaleel, H., Ahmad, B., Raina, A., Jaleel, H., Ahmad, B., Raina, A., Khan, F.A., Naushin, F., 2019. Role and regulation of plants phenolics in abiotic stress tolerance: an overview. editors. In: Khan, M.I.R., Reddy, P.S., Ferrante, A., Khan, N.A. (Eds.), Plant Signaling Molecules. Elsevier, Amsterdam, The Netherlands, pp. 157–168.
Nakano, Y., Asada, K., 1981. Hydrogen peroxide is scavenged by ascorbate-specific peroxidase in spinach chloroplasts. Plant Cell Physiol. 22 (5), 867–880. https://doi.org/10.1093/oxfordjournals.pcp.a076232.
Navrátil, M., Špunda, V., Marková, I., Janouš, D., 2007. Spectral composition of photosynthetically active radiation penetrating into a Norway spruce canopy: the opposite dynamics of the blue/red spectral ratio during clear and overcast days. Trees 21 (3), 311–320.
Osunkoya, O.O., Ash, J.E., Hopkins, M.S., Graham, A.W., 1994. Influence of seed size and seedling ecological attributes on shade-tolerance of rain-forest tree species in northern Queensland. J. Ecol. 149–163. https://doi.org/10.2307/2261394.
Pantera, A., Mosquera-Losada, M.R., Herzog, F., Den Herder, M., 2021. Agroforestry and the environment. Agrofor. Syst. 95 (5), 767–774.
Poorter, H., Fiorani, F., Pieruschka, R., Wojciechowski, T., van der Putten, W.H., Kleyer, M., Schurr, U., Postma, J., 2016. Pampered inside, pestered outside? Differences and similarities between plants growing in controlled conditions and in the field. New Phytol. 212 (4), 838–855.
Poorter, H., Niinemets, Ü., Ntagkas, N., Siebenkäs, A., Mäenpää, M., Matsubara, S., Pons, T., 2019. A meta-analysis of plant responses to light intensity for 70 traits ranging from molecules to whole plant performance. New Phytol. 223 (3), 1073–1105.
Poorter, H., Niinemets, Ü., Poorter, L., Wright, I.J., Villar, R., 2009. Causes and consequences of variation in leaf mass per area (LMA): a meta-analysis. New Phytol. 182 (3), 565–588.
Poorter, L., 1999. Growth responses of 15 rain-forest tree species to a light gradient: the relative importance of morphological and physiological traits. Funct. Ecol. 13 (3), 396–410. https://doi.org/10.1046/j.1365-2435.1999.00332.x.
Pospisil, P., 2016. Production of reactive oxygen species by photo system II as a response to light and temperature stress. Front. Plant Sci. 7, 1950. https://doi.org/10.3389/fpls.2016.01950.
Qaderi, M.M., Martel, A.B., Strugnell, C.A., 2023. Environmental factors regulate plant secondary metabolites. Plants 12 (3), 447.
Rodríguez-López, N.F., Martins, S.C.V., Cavatte, P.C., Silva, P.E.M., Morais, L.E., Pereira, L.F., Reis, J.V., Ávila, R., Godoy, A.G., Lavinski, A.O., DaMatta, F.M., 2014. Morphological and physiological acclimations of coffee seedlings to growth over a range of fixed or changing light supplies. Env. Exp. Bot. 102, 1–10.
Sanford, N.L., Harrington, R.A., Fownes, J.H., 2003. Survival and growth of native and alien woody seedlings in open and understory environments. For. Ecol. Manag. 183 (1–3), 377–385.

Sheu, Y.W., Chiang, L.C., Chen, I.S., Chen, Y.C., Tsai, I.L., 2005. Cytotoxic flavonoids and new chromenes from *Ficus formosana* f. *formosana*. Planta Med. 71 (12), 1165–1167.
Simkin, A.J., Kapoor, L., Doss, C.G.P., Hofmann, T.A., Lawson, T., Ramamoorthy, S., 2022. The role of photosynthesis related pigments in light harvesting, photoprotection and enhancement of photosynthetic yield in planta. Photosyn. Res. 152 (1), 23–42.
Singleton, V.L., Rossi, J.A., 1965. Colorimetry of total phenolics with phosphomolybdic-phosphotungstic acid reagents. Am. J. Enol. Vitic. 16 (3), 144–158.
Szymańska, R., Ślesak, I., Orzechowska, A., Kruk, J., 2017. Physiological and biochemical responses to high light and temperature stress in plants. Env. Exp. Bot. 139, 165–177.
Telfer, A., 2014. Singlet oxygen production by PSII under light stress: mechanism, detection and the protective role of β-carotene. Plant Cell Physiol. 55 (7), 1216–1223.
Thitisaksakul, M., Dong, S., Beckles, D.M., 2017. How rice glycogen synthase kinase-like 5 (OsGSK5) integrates salinity stress response to source-sink adaptation: a proposed model. Plant Signal. Behav. 12 (12), e1403708.
Tzeng, H.Y., Tzeng, L.J., Ou, C.H., Lu, F.Y., 2005. Phenology of *Ficus formsana* Maxim. At Guandaushi forest ecosystem. Q. J. For. Res. 38 (4), 377–395 [in Chinese with English summary]. https://doi.org/10.30064/QJCF.200512.0001.
Valladares, F., Gianoli, E., Gómez, J.M., 2007. Ecological limits to plant phenotypic plasticity. New Phytol. 176 (4), 749–763.
Valladares, F., Laanisto, L., Niinemets, Ü., Zavala, M.A., 2016. Shedding light on shade: ecological perspectives of understorey plant life. Plant Ecol. Divers. 9 (3), 237–251.
Wang, D., Huang, X., Chen, J., Li, L., Cheng, J., Wang, S., Liu, J., 2021. Plasticity of leaf traits of *Juglans regia* L. f. *luodianense* Liu et Xu seedlings under different light conditions in Karst habitats. Forests. 12 (1), 81.
Willekens, H., Chamnongpol, S., Davey, M., Schraudner, M., Langebartels, C., Van Montagu, M., Inzé, D., Van Camp, W., 1997. Catalase is a sink for H_2O_2 and is indispensable for stress defence in C3 plants. EMBO J. 16 (16), 4806–4816. https://doi.org/10.1093/emboj/16.16.4806.
Wu, C.C., Lin, Y.R., Liu, W.Y., 2020. Evaluating the cost-effectiveness of shaded-agroforestry economic crops in the forestlands. Q. J. For. Res. 42 (2), 105–117 [in Chinese with English summary]. https://www.airitilibrary.com/Article/Detail?DocID=16068351-202006-202008260010-202008260010-105-117.
Wyka, T., Oleksyn, J., Zytkowiak, R., Karolewski, P., Jagodziński, A., Reich, P., 2012. Responses of leaf structure and photosynthetic properties to intra-canopy light gradients: a common garden test with four broadleaf deciduous angiosperm and seven evergreen conifer tree species. Oecologia 170, 11–24.
Xu, Y.R., 2019. The next step in the under-forest economy. For. Res. Newsl. 26 (5), 58–61 [in Chinese]. https://www.airitilibrary.com/Article/Detail?DocID=16056922-201910-201911130005-201911130005-58-61.
Xu, F.J., Li, G., Jin, C.W., Liu, W.J., Zhang, S.S., Zhang, Y.S., Lin, X.Y., 2012. Aluminum-induced changes in reactive oxygen species accumulation, lipid peroxidation and antioxidant capacity in wheat root tips. Biol. Plant 56, 89–96.
Xu, Y., Wang, G., Cao, F., Zhu, C., Wang, G., El-Kassaby, Y.A., 2014. Light intensity affects the growth and flavonol biosynthesis of Ginkgo (*Ginkgo biloba* L.). New. For. 45, 765–776.
Young, K.J., 2017. Mimicking nature: a review of successional agroforestry systems as an analogue to natural regeneration of secondary forest stands. In: Montagnini, F. (Ed.), Integrating Landscapes: Agroforestry for Biodiversity Conservation and Food Sovereignty. Advances in Agroforestry, Integrating Landscapes: Agroforestry for Biodiversity Conservation and Food Sovereignty. Advances in Agroforestry, 12. Springer, Cham.